Novel Pressure-induced Phenomena in Condensed Matter Systems
J. Phys. Soc. Jpn. **76** (2007) Suppl. A, pp. 27-30

Excitonic versus electron-hole liquid phases in Tm[Se,Te] compounds

Franz X. Bronold[1]*, Holger Fehske[1], and Gerd Röpke[2]

[1]*Institut für Physik, Ernst-Moritz-Arndt-Universität Greifswald, D-17489 Greifswald, Germany*
[2]*Fachbereich Physik, Universität Rostock, D-18051 Rostock, Germany*

(Received July 25, 2006)

We discuss, from a theoretical point of view, excitonic phases at the pressure induced semiconductor-semimetal transition in $TmSe_{0.45}Te_{0.55}$, focusing, in particular, on the stability against an electron-hole liquid. The electron-hole pair density parameter $r_s(E_g, T)$ is calculated within the quasi-static plasmon pole approximation as a function of temperature T and energy gap E_g and converted into $-E_g(r_s, T)$. A comparison of this quantity, which is the electron-hole pair chemical potential, with the exciton binding energy reveals that excitons should be suppressed in contrast to experimental evidence for excitonic phases. We suspect therefore inter-valley exciton scattering and exciton-phonon scattering to substantially stabilise excitons in $TmSe_{0.45}Te_{0.55}$.

KEYWORDS: semiconductor-semimetal transition, electron-hole liquids, exciton condensation

1. Introduction

The possibility of an excitonic insulator – understood as a macroscopic, phase coherent quantum state (exciton condensate) – separating below a critical temperature a semiconductor (SC) from a semimetal (SM), has been anticipated by theorists long time ago.[1)] Experimental efforts, however, to establish this phase in real compounds largely failed. The most promising candidates so far are the hexaborides,[2)] where the unexpected ferromagnetism may be interpreted in terms of a doped excitonic insulator,[3,4)] and $TmSe_{0.45}Te_{0.55}$, where the unusual thermal diffusivity may be due to a superfluid exciton state.[5)]

We focus on $TmSe_{0.45}Te_{0.55}$. In a series of experiments, Wachter and coworkers compiled strong evidence for excitonic phases in the vicinity of the pressure-induced SC-SM transition in $TmSe_{0.45}Te_{0.55}$.[5–7)] In particular, the anomalous increase of the electrical resistivity in a narrow pressure range around 8 kbar indicated the appearance of a new phase below 250 K. Wachter and coworkers suggested that this new phase might be an "excitonic insulator", and, assuming the energy gap E_g to decrease with increasing pressure, constructed a phase diagram for $TmSe_{0.45}Te_{0.55}$ in the $E_g - T$ plane.[6)] Later they found in the same material a linear increase of the thermal diffusivity below 20 K and related this to a superfluid exciton state.[5)] Both excitonic phases are located on the SC side of the SC-SM transition in $TmSe_{0.45}Te_{0.55}$.

In our previous work[8)] we presented a theoretical analysis of these astonishing experimental findings. We calculated for a model mimicking the situation in $TmSe_{0.45}Te_{0.55}$ the phase boundary $T_c(E_g)$ for an excitonic insulator and investigated the composition of its environment. Our main conclusions were: (i) The phase boundary constructed from the resistivity data does not embrace the excitonic insulator. Instead, it most probably traces the exciton-rich region above an excitonic insulator, where excitons dominate the total density, provide abundant scattering centres for the charge carriers, and induce the observed resistivity anomaly. (ii) The linear increase of the thermal diffusivity below 20 K, on the other hand, could signal exciton condensation. The large electron-hole mass asymmetry places the excitonic insulator entirely on the SC side, where it is supported by strongly bound, bosonic excitons. A transition to a superfluid state, similar to the transition in liquid He 4, is thus conceivable and could give rise to the observed atypical thermal diffusion.

We based our calculation on an effective-mass, Wannier-type model for electrons in the lowest conduction band (CB) and holes in the highest valence band (VB), with an indirect energy gap separating the two bands, a multiplicity factor to account for three equivalent CB minima arising from the fcc crystal structure of $TmSe_{0.45}Te_{0.55}$, and a statically screened Coulomb potential operating between the constituents of the model (in contrast to the quasi-static screening model used below). Because of the limitations of the model, which, for instance, neglects lattice effects, we could not obtain complete quantitative agreement between theory and experiment. Yet, our results indicate that Wachter and coworkers[5–7)] may have seen an exciton condensate.

Clearly, within an effective electron-hole model quantitative agreement between experiment and theory cannot be expected. Instead of augmenting the model with additional degrees of freedom, we still want to stay in the present paper within its bounds and discuss the possibility of an electron-hole liquid[9)] which competes with excitonic phases in materials where the band structure is multi-valleyed. The results will further benchmark the model and thus guide its modification.

2. Method

The thermodynamics of an electron-hole liquid is contained in the electron-hole pair chemical potential $\mu_{eh}(r_s, T)$ which depends on the electron-hole pair density parameter r_s and the temperature T.[9)] In our case, $\mu_{eh} = -E_g$, with E_g the energy gap fixed by the external pressure. Therefore, we first have to determine $r_s(E_g, T)$ and then convert this relation into $-E_g(r_s, T)$.

*E-mail address: bronold@physik.uni-greifswald.de

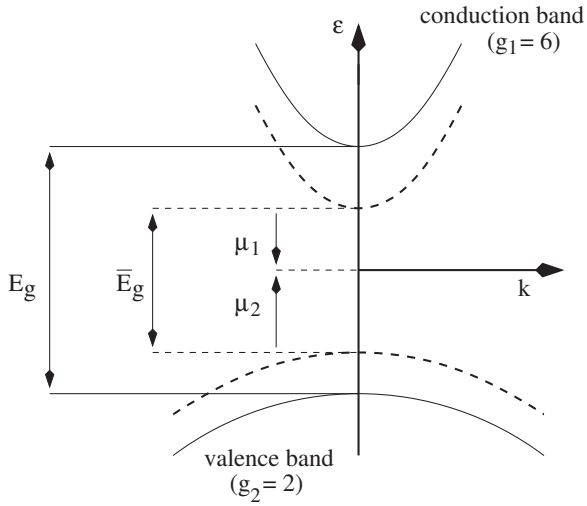

Fig. 1. The band structure of the effective-mass, Wannier-type model. We measure momenta $\mathbf{k}$ for the CB electrons and VB holes from the respective extrema of the bands which, in reality, are separated by $\mathbf{w} = \mathbf{K}/2$ where $\mathbf{K}$ is the reciprocal lattice vector connecting the Γ with the X points of the Brillouin zone for a fcc lattice. The energy gap E_g varies continuously through zero under pressure. Solid (dashed) parabola denote the bare (renormalised) energy bands. Note, the auxiliary chemical potentials μ_i are defined with respect to the shifted band edges. The factors g_i account for spin and the number of equivalent valleys.

Comparing $-E_g(r_s, T)$ with the exciton binding energy and analysing for fixed temperature its r_s-dependence enables us to determine the region in the $E_g - T$ plane where an electron-hole liquid may be favoured over excitonic phases. We calculate $-E_g(r_s, T)$ in the quasi-static plasmon-pole approximation.[10)]

The schematic band structure used in Ref.[8)] to model $TmSe_{0.45}Te_{0.55}$ is shown in Fig. 1. Within the quasi-static plasmon-pole approximation the CB electron ($i = 1$) and VB hole ($i = 2$) selfenergies, leading, at finite filling, to the renormalization of the energy bands (dashed parabola in Fig. 1), can be written as

$$\Sigma_i(\mathbf{k}) = \Sigma_i^{sx}(\mathbf{k}) + \Sigma_i^{ch}(\mathbf{k}) \ , \tag{1}$$

where the first term,

$$\Sigma_i^{sx}(\mathbf{k}) = -\sum_{\mathbf{k}'} V_s(\mathbf{k}-\mathbf{k}') n_{\rm F}(\epsilon_i(\mathbf{k}') - \mu_i) \ , \tag{2}$$

denotes the exchange energy and the second,

$$\Sigma_i^{ch}(\mathbf{k}) = \frac{1}{2}\sum_{\mathbf{k}'} \big[V_s(\mathbf{k}') - V_0(\mathbf{k}')\big] \ , \tag{3}$$

the Coulomb-hole energy. Here, $V_0(\mathbf{q}) = 4\pi e^2/\varepsilon_0 q^2$ is the Coulomb potential reduced by the background dielectric constant ε_0, $V_s(\mathbf{q})$ is the statically screened Coulomb potential to be defined below, $\epsilon_i(\mathbf{k}) = \mathbf{k}^2/2m_i$ (m_i are the effective masses), and $n_{\rm F}(\epsilon)$ is the Fermi function. In contrast to the static approximation used in Ref.,[8)] which replaces directly in the Hamiltonian $V_0(\mathbf{q})$ by $V_s(\mathbf{q})$, the selfenergies contain now not only the exchange corrections but also the Coulomb-hole.

The screened Coulomb potential in Eqs. (2) and (3) is the static limit of the dynamically screened Coulomb potential,

$$V_s(\mathbf{q}) \equiv V_s(\mathbf{q}, 0) = V_0(\mathbf{q})/\varepsilon(\mathbf{q}, 0) \ , \tag{4}$$

where the dielectric function is given by

$$\frac{1}{\varepsilon(\mathbf{q},\omega)} = 1 + \frac{\omega_{pl}^2}{(\omega + i\eta)^2 - \omega(\mathbf{q})^2} \ , \tag{5}$$

with an effective plasmon dispersion,

$$\omega(\mathbf{q})^2 = \omega_{pl}^2\big[1 + \big(\frac{q}{q_s}\big)^2\big] + C\big(\frac{q^2}{4m_1} + \frac{q^2}{4m_2}\big)^2 \ , \tag{6}$$

constructed in such a way that sum rules are satisfied.[10)] When the plasmon-pole approximation is constructed from the Lindhard dielectric function, the coefficient $C = 1$. It can be however also used as a fit parameter to correct for the overestimation of screening within the quasi-static approximation. In that case $1 \le C \le 4$.[10)] The screening wave number,

$$q_s = \sqrt{\frac{4\pi e^2}{\varepsilon_0}\big[\frac{\partial}{\partial\mu_1} n_1 + \frac{\partial}{\partial\mu_2}\bar{n}_2\big]} \ , \tag{7}$$

and plasma frequency,

$$\omega_{pl} = \sqrt{\frac{4\pi e^2}{\varepsilon_0}\big[\frac{n_1}{m_1} + \frac{\bar{n}_2}{m_2}\big]} \ , \tag{8}$$

entering Eq. (6) depend on the CB electron and VB hole densities given, respectively, by

$$n_1 = g_1 \sum_{\mathbf{k}} n_{\rm F}(\epsilon_1(\mathbf{k}) - \mu_1) \ , \tag{9a}$$

$$\bar{n}_2 = g_2 \sum_{\mathbf{k}} n_{\rm F}(\epsilon_2(\mathbf{k}) - \mu_2) \ , \tag{9b}$$

where the multiplicity factors g_i contain the spin and the number of equivalent valleys.

The main effect of the selfenergies Σ_i is a rigid, $\mathbf{k}$-independent shift of the single particle dispersions leading to a renormalised band gap $\bar{E}_g$. This situation has been anticipated in Eqs. (2), (9a), and (9b), where we introduced auxiliary chemical potentials μ_i, measured from the shifted band edges (see Fig. 1). By construction,

$$\mu_1 + \mu_2 = -\bar{E}_g \ . \tag{10}$$

The bare energy gap E_g, that is, the parameter which is experimentally controlled via pressure, is given by

$$E_g = \bar{E}_g - \Sigma_1(0) - \Sigma_2(0) \ . \tag{11}$$

Supplementing Eqs. (10) and (11) with the condition of charge neutrality,

$$n_1 = \bar{n}_2 \ , \tag{12}$$

we obtain a closed set of equations for the three unknown parameters μ_1 and μ_2, and $\bar{E}_g$.

To construct from Eqs. (10) – (12) the electron-hole pair chemical potential $-E_g(r_s, T)$, we proceed as follows: First, we calculate from Eqs. (12), (10), (9b) and (9a), the auxiliary chemical potentials μ_i as a function of $\bar{E}_g$ and T. Inserting $\mu_i(\bar{E}_g, T)$ in Eqs. (7) and (8), we obtain $q_s(\bar{E}_g, T)$ and $\omega_{pl}(\bar{E}_g, T)$, which enables us to determine V_s and thus the selfenergies Σ_i in the whole $\bar{E}_g - T$ plane. Via Eq. (11) we then obtain the important relation

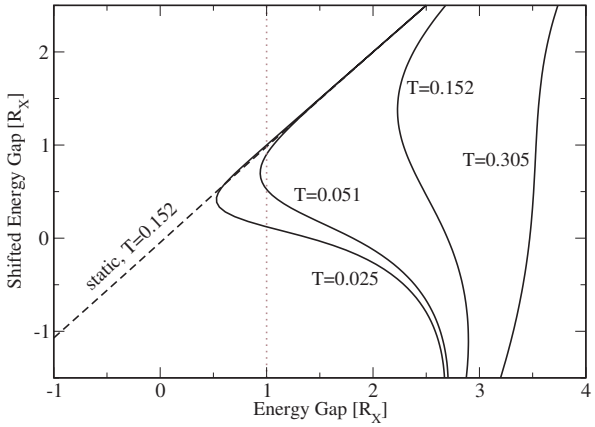

Fig. 2. Shifted energy gap $\bar{E}_g$ as a function of the pressure-tuned energy gap E_g and temperature T for $TmSe_{0.45}Te_{0.55}$ parameters: $\alpha = 0.015$, $g_1 = 6$, and $g_2 = 2$. The dotted line denotes the energy where the excitonic instability would occur at $T = 0$ and the dashed line gives $\bar{E}_g(E_g, T = 0.152)$ in the static approximation.

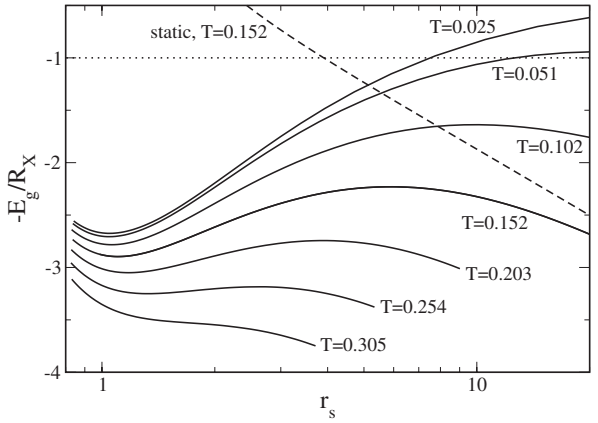

Fig. 3. Electron-hole pair chemical potential $-E_g(r_s, T)$ as a function of electron-hole pair density parameter r_s and temperature T for $TmSe_{0.45}Te_{0.55}$ parameters: $\alpha = 0.015$, $g_1 = 6$, and $g_2 = 2$. The dotted line indicates where the excitonic instability would occur at $T = 0$ and the dashed line gives $-E_g(r_s, T = 0.152)$ in the static approximation. Note, for $T < 0.305$, the isotherms go through a minimum.

$E_g(\bar{E}_g, T)$. Finally, we use either Eq. (9a) or Eq. (9b) to map, for a given temperature T, the renormalised energy gap $\bar{E}_g$ on to the electron-hole pair density $n \equiv n_1 = \bar{n}_2$. Using the density parameter $r_s = (3/4\pi n \cdot a_X^3)^{1/3}$, with a_X the exciton Bohr radius defined in the next section, instead of the pair density, we find $-E_g(r_s, T)$.

3. Results

In the following, we measure energies and lengths in units of the exciton Rydberg $R_X = 1/2ma_X^2$ and the exciton Bohr radius $a_X = \varepsilon_0/me^2$, respectively ($\hbar = 1$). The model shown in Fig. 1 is then completely specified by the multiplicity factors g_i and the effective mass ratio $\alpha = m_1/m_2$. For $TmSe_{0.45}Te_{0.55}$ the corresponding values are $g_1 = 6$, $g_2 = 2$, and $\alpha \approx 0.015$.[5,8] Due to the lack of data about band gap renormalization in $TmSe_{0.45}Te_{0.55}$, we cannot use C in Eq. (6) as a fit parameter. Thus, $C = 1$, which almost certainly overestimates screening.

The shifted energy gap $\bar{E}_g$ as a function of the energy gap E_g is shown in Fig. 2 for several temperatures. First we note the drastic difference to the static approximation ($V_0 \to V_s$ in the Hamiltonian). Whereas in the static approximation $\bar{E}_g$ decreases monotonously with E_g for all temperatures, the quasi-static approximation gives, for some E_g-range, a triple-valued $\bar{E}_g$ for $T < 0.305$. Because of the one-to-one correspondence between $\bar{E}_g$ and the pair density n, this means the system cannot choose a unique pair density. As a consequence, there may be parts in the $\bar{E}_g - T$-plane where an electron-hole gas coexists with an electron-hole liquid. Note, the renormalised band gap $\bar{E}_g$ resembles the selfenergy parameter S introduced before to set up a Hartree-Fock description of the gas/liquid transition in a generic electron-hole plasma.[12]

The corresponding pair chemical potential $-E_g(r_s, T)$ is shown in Fig. 3. Various subtle points should be noticed before we can attempt an interpretation of the data. First, $-E_g(r_s, T)$ does not asymptotically merge with the exciton Rydberg for $r_s \to \infty$. Thus, the results in the extreme dilute limit are flawed, not only in the quasi-static approximation (solid lines) but also in the static approximation (dashed line). This is a well-known shortcoming of random-phase-approximation based screening models, which neglect multiple-scattering between charged carriers. Including multiple-scattering (ladder diagrams) in the quasi-static (static) approximation would force the chemical potential $-E_g(r_s, T)$ to approach for $r_s \to \infty$ the exciton Rydberg from below (above). Second, the densities of interest are rather low ($r_s \gtrsim 1$). Corrections due to multiple scattering are therefore not necessarily small and should be included, a formidable task beyond the scope of the present paper.

With these caveats in mind we now extract the physical implications of the data shown in Fig. 3. As expected from the $\bar{E}_g$-isotherms, the model shown in Fig. 1 yields for $TmSe_{0.45}Te_{0.55}$ parameters a chemical potential which shows the typical van-der-Waals behaviour: Above a critical temperature ($T_{crit} \approx 0.254$), the chemical potential increases monotonously with density (recall: $r_s \sim 1/n^{1/3}$). Below the critical temperature, the chemical potential has a local maximum and a local minimum. This can be most clearly seen from the $T = 0.203$ isotherm. A Maxwell construction would thus give the equilibrium chemical potential and the coexistence region between the gaseous and the liquid phases. Anticipating however the correct dilute limit, a Maxwell construction cannot be made and the minimum simply indicates a jump in the pair densities, that is, for large enough energy gaps the pair density n drops to zero.[11] Only when the exciton binding energy is below the minimum of the chemical potential, a gas/liquid transition and with it a coexistence region could appear. In that case, excitons would be also stable in a certain range. Because of the experimental evidence for excitonic phases, we expect this situation to be actually realised in $TmSe_{0.45}Te_{0.55}$.

The minimum of the pair chemical potential

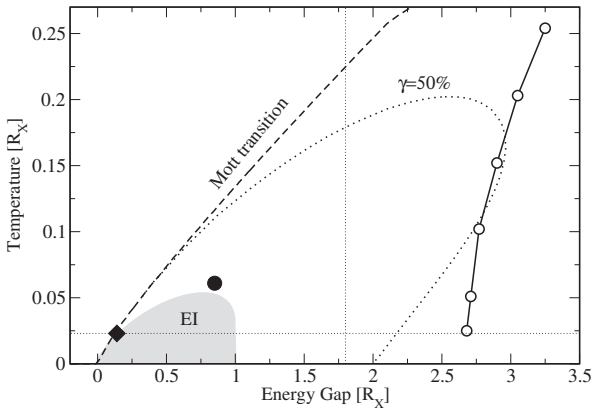

Fig. 4. Phase boundaries obtained for $TmSe_{0.45}Te_{0.55}$ parameters: $\alpha = 0.015$, $g_1 = 6$, and $g_2 = 2$. The thick dotted line is the 50%-contour of the bound state fraction γ.[8] Beyond the dashed line excitons disappear because of the Mott effect and the grey region denotes the excitonic insulator (EI).[8] At the full diamond on the horizontal thin dotted line the linear increase of the thermal diffusivity has been experimentally found[5] and at the full circle $n_1^b \approx 1.3 \times 10^{21}$ cm^{-3}[8] in good agreement with the experimentally estimated exciton density 3.9×10^{21} cm^{-3}.[7] The open circles are the points where $-E_g(r_s, T)$ goes through the minimum. The energy gap of $TmSe_{0.45}Te_{0.55}$ at ambient pressure is given by the vertical thin dotted line.

$-E_g(r_s, T)$ is below the exciton Rydberg. Therefore, taking the correct $r_s \to \infty$ limit of $-E_g(r_s, T)$ into account, our results for the pair chemical potential suggest that in the Wannier-type model excitons and thus excitonic phases (exciton gas, excitonic insulator) are unstable against a metallic phase. Anticipating, in addition, the decrease of the exciton binding energy with increasing density, the metallic phase would be in fact favoured over most of the relevant parameter range discussed in Ref.[8] and in stark contrast to the experimentally observed increase of the resistivity.

This can be seen in Fig. 4 which combines the points where $-E_g(r_s, T)$ is minimal with (i) the phase boundary of the excitonic insulator, (ii) the 50%-contour of the bound state fraction $\gamma = n_1^b/(n_1^f + n_1^b)$ (n_1^f and n_1^b are the free and the bound part of the total density obtained from a T-matrix calculation of the total density), and (iii) the Mott line beyond which excitons disappear because Pauli blocking and screening lead to a vanishing exciton binding energy. All of it has been calculated in Ref.[8] within the static screening model. We expect however the quasi-static approximation to give similar results.

One of our main conclusions in Ref.[8] was that the resistivity anomaly, that is, the experimentally observed increase of the resistivity in a narrow pressure range, is most probably due to exciton-electron and exciton-hole scattering which would be very efficient above an excitonic insulator. Indeed, the temperature range, where the 50%-contour is located, coincides roughly with the temperature range where the anomaly has been detected. In contrast, the analysis of the pair chemical potential performed in this paper suggests excitons in that region to be unstable against a metallic electron-hole plasma. An increase of the resistivity is however hard to reconcile with a metallic phase. We expect therefore excitons in $TmSe_{0.45}Te_{0.55}$ to be stabilised by band structure effects beyond the model shown in Fig. 1 and additional scattering processes. That the effective-mass, Wannier-type model may not be quite adequate can be also seen from the fact that the experimentally determined exciton Rydberg for $TmSe_{0.45}Te_{0.55}$ is ≈ 75 meV whereas the energy gap at ambient pressure is ≈ 135 meV and thus only $\approx 1.8 \cdot R_X$ (vertical thin dotted line in Fig. 4).

In analogy to the hexaborides,[11] we expect coherent inter-valley scattering of excitons to increase the exciton binding energy. Additionally, exciton-phonon scattering should also increase the binding energy of an exciton in $TmSe_{0.45}Te_{0.55}$ because the narrow VB makes the exciton very susceptible to phonon dressing. In fact, there is plenty of experimental evidence for strong exciton-phonon coupling in $TmSe_{0.45}Te_{0.55}$.[5] Both scattering processes should be studied in detail, ideally in a model which avoids the effective mass approximation and keeps the full band structure. If it turns out that in a more realistic model the exciton binding energy is still above the chemical potential of the metallic phase, excitonic phases must be ruled out in $TmSe_{0.45}Te_{0.55}$. On the other hand, if the exciton binding energy is pushed below the minimum of the metallic chemical potential, and that is not unrealistic considering the energy gain coherent inter-valley scattering alone can yield if the band structure permits it,[11] excitons are stable, at least in some pressure range, and the excitonic instability leading to an excitonic insulator could take place in $TmSe_{0.45}Te_{0.55}$ before an electron-hole gas-liquid transition interferes.

Acknowledgment

Support from the SFB 652 is greatly acknowledged. We thank D. Ihle for valuable discussions.

1) For a review, see B. I. Halperin and T. M. Rice in: *Solid State Physics*, eds. F. Seitz, D. Turnbull, and H. Ehrenreich (Academic Press, New York, 1968) Vol. **21**, pp. 115.
2) D. P. Young, D. Hall, M. E. Torelli, Z. Fisk, J. L. Sarrao, J. D. Thompson, H.-R. Ott, S. B. Oseroff, R. G. Goodrich, and R. Zysler: Nature **397** (1999) 412.
3) M. E. Zhitomirsky, T. M. Rice, and V. I. Anisimov: Nature **402** (1999) 251.
4) E. Bascones, A. A. Burkov, and A. H. MacDonald: Phys. Rev. Lett. **89** (2002) 086401.
5) P. Wachter, B. Bucher, and J. Malar: Phys. Rev. B **69** (2004) 094502.
6) J. Neuenschwander and P. Wachter: Phys. Rev. B **41** (1990) 12693; B. Bucher, P. Steiner, and P. Wachter: Phys. Rev. Lett. **67** (1991) 2717.
7) P. Wachter: Solid State Commun. **118** (2001) 645.
8) F. X. Bronold and H. Fehske, Phys. Rev. B **74** (2006) 165107.
9) For a review, see T. M. Rice in: *Solid State Physics*, eds. F. Seitz, D. Turnbull, and H. Ehrenreich (Academic Press, New York, 1977), Vol. **32**, pp. 1.
10) H. Haug and S. Schmitt-Rink: Prog. Quant. Electr. **9** (1984) 3.
11) M. E. Zhitomirsky and T. M. Rice: Phys. Rev. B **62** (2000) 1492.
12) R. N. Silver: Phys. Rev. B **8** (1973) 2403.